Reaction Mechanisms in Both a $CHF_3/O_2/Ar$ and $CHF_3/H_2/Ar$ Radio Frequency Plasma Environment

Ya-Fen Wang,*,† Wen-Jhy Lee,† Chuh-Yung Chen,*,‡ and Lien-Te Hsieh†

Departments of Environmental Engineering and Chemical Engineering, National Cheng Kung University, No. 1, University Road, Tainan 70101, Taiwan

A radio frequency (RF) plasma system used to decompose trifluoromethane (CHF_3 or HFC-23) is demonstrated. The CHF_3 decomposition fractions (η_{CHF_3}) and mole fractions of detected products in the effluent gas streams of $CHF_3/O_2/Ar$ and $CHF_3/H_2/Ar$ plasma systems, respectively, have been determined. The effects of four experimental parameters, input power, O_2/CHF_3 or H_2/CHF_3 ratio, operational pressure, and the CHF_3 feeding concentration were investigated. The same species detected in the effluent gas streams of both $CHF_3/O_2/Ar$ and $CHF_3/H_2/Ar$ plasma systems were CH_2F_2, CF_4, HF, and SiF_4. However, the CO_2 and COF_2 were detected only in the $CHF_3/O_2/Ar$ plasma system and the CH_4, C_2H_2, and CH_3F were detected only in the $CHF_3/H_2/Ar$ plasma system. The results of a model sensitivity analysis showed that the input power was the most influential parameter for η_{CHF_3} both in the $CHF_3/O_2/Ar$ and $CHF_3/H_2/Ar$ plasma systems. Furthermore, the possible reaction pathways were built up and elucidated in this study. The addition of hydrogen for CHF_3 decomposition can produce a significant amount of HF and the main carbonaceous byproducts were CH_4 and C_2H_2. Even though the η_{CHF_3} in the $CHF_3/H_2/Ar$ plasma system is lower than that in the $CHF_3/O_2/Ar$ plasma system, but due to the more advantages mentioned above, a hydrogen-based RF plasma system is a better alternative to decompose CHF_3.

1. Introduction

Fluorocompounds (FCs) were most known as fire suppressants,[1,2] chemical extinguishers[3] and ozone-depleting substances.[4,5] Today, various FCs have been applied in the semiconductor industry, such as chemical vapor deposition (CVD) techniques[6,7] and chemical-etching processes.[8,9] Typically, gaseous effluents which contained various FCs emitting from these processes were diluted with vast quantities of air or nitrogen and were either released into the atmosphere or thermally incinerated.[10] Some FCs are atmospherically long-lived, strong infrared absorbers,[11] and thermally stable.[10] These compounds are not effectively treated by the incineration process, raising issues about environmental impact and climate change concerns.[11]

Great attention has been focused on the control and reduction of perfluorocompounds (PFCs) emissions, especially for the semiconductor industry. The control technologies of PFCs emissions include process optimization, PFC replacement, PFC capture/recovery, and destructive abatement.[11] In general, the CVD processes or the dry-etching processes are typically parameter-adjusted and end-pointed to meet the regulated requirements, and there may be little opportunity to further optimize the processes to reduce the PFCs emissions.[11] In addition, some studies are focused on membrane systems for PFCs capture and recovery.[12] But the exhausts containing HF and SiF_4 chemically degraded the membrane and particulates presented in the stream physically blocked the pore sites. Furthermore, PFCs destruction efficiency in a combustion system generally follows the PFCs' thermodynamic stabilities, making CF_4 abatement a particular challenge.[11]

Radio frequency (RF) plasma technology provides a more complete and lower temperature reaction environment for gas molecules than other methods do. It was a branch of nonequilibrium plasma which was often referred to as cold plasma.[13] The kinetic energy of electrons and ions is higher than that of molecules in the cold plasma system. In general, the apparent operating temperature in the RF plasma reactor is lower than 400 °C. However, the real temperature of electrons in the RF plasma reactor is higher than 2000 °C.[14] Therefore, conventional reaction which needs to proceed at a very high temperature can be finished at a lower temperature in the cold plasma system.[15] This technology can act directly on the process stream and become part of the tool outlet piping. It will avoid the problem of nitrogen dilution and the space requirements are minimal compared with those of the combustion method.

Trifluoromethane (CHF_3, HFC-23), widely used for dielectric film etching, fire extinguishment agents to replace Halon 1301 and CFC replacements for refrigeration,[16] is the simplest PFC. Furthermore, CHF_3 was also evaluated as a supercritical fluid extractant.[17] The various applications of CHF_3 made it interesting to understand the reaction mechanisms in the RF plasma system. In this study, the model sensitivity analysis was employed[18] for studying the effects of experimental parameters, the input power, O_2/CHF_3 or H_2/CHF_3 ratio, operational pressure, and CHF_3 feeding concentration, on the CHF_3 decomposition fraction (η_{CHF_3}) and the fraction of total-carbon input converted into CO_2 (F_{CO_2}) or $CH_4+C_2H_2$ ($F_{CH_4+C_2H_2}$) in the $CHF_3/O_2/Ar$ and $CHF_3/H_2/Ar$ plasma system, respectively. The η_{CHF_3} and the mole fractions of detected products in these two plasma

* To whom correspondence should be addressed. Tel.: 886-6-275-7575, ext. 54531. Fax: 886-6-275-2790. E-mail: wjlee@mail.ncku.edu.tw.

† Department of Environmental Engineering.

‡ Department of Chemical Engineering.

10.1021/ie9900519 CCC: $18.00
Published on Web 08/19/1999

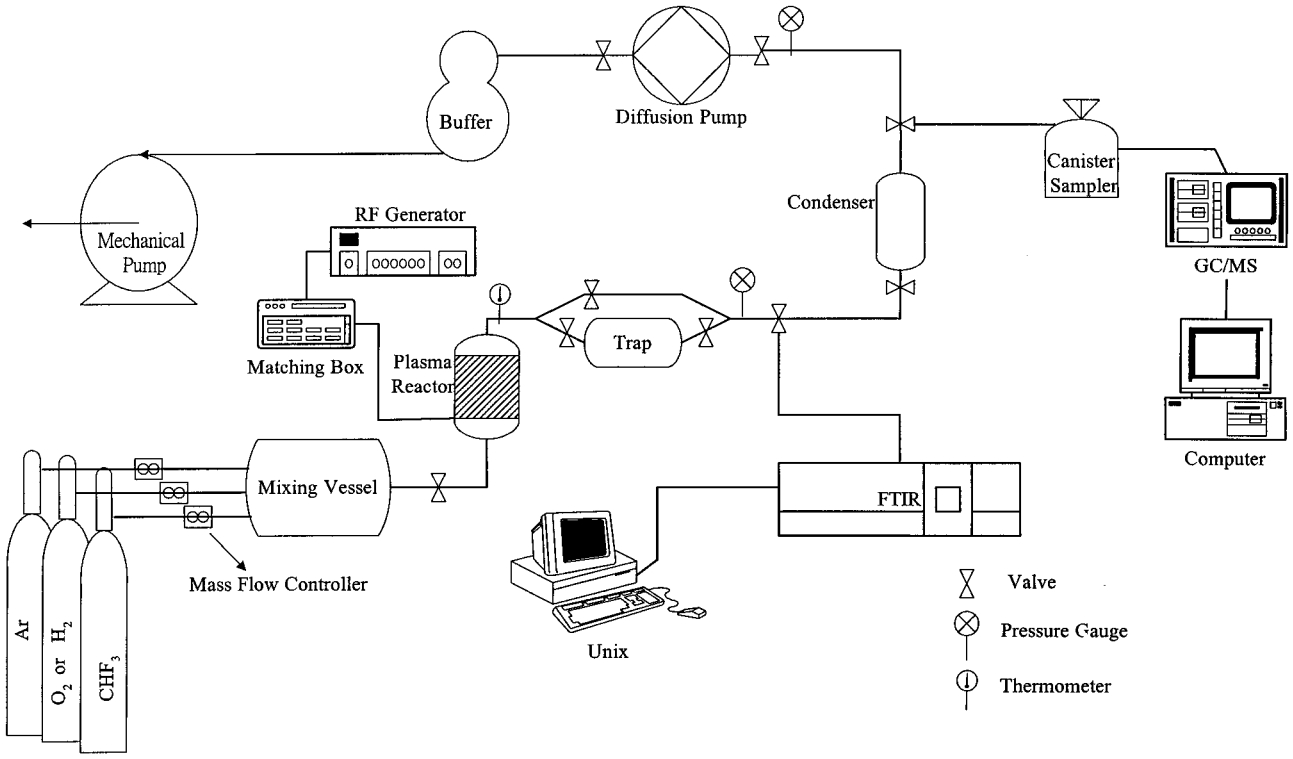

Figure 1. Schematic of the RF plasma system.

systems were compared and discussed. Finally, the possible reaction pathways in the $CHF_3/O_2/Ar$ and $CHF_3/H_2/Ar$ plasma reactor were elucidated, respectively.

2. Experimental Description

2.1. Experimental Analysis. Figure 1 schematically showed the experimental apparatus used in this study. The $CHF_3/O_2/Ar$ or $CHF_3/H_2/Ar$ mixing gas was metered using Brooks-type 5850E mass flow controllers at a total flow rate of 100 sccm (cm^3/min, 1 atm−273 K) that entered a mixing vessel and were introduced perpendicularly into a 4.14 cm (i.d.) × 15 cm (height) cylindrical glass reactor. The RF plasma discharge was produced using a plasma generator (PFG 600 RF, Fritz Huttinger Elektronik Gmbh) at 13.56 MHz and with a matching network (Matchbox PFM). The RF power was delivered through the power meter and the matching unit to an outer copper electrode wrapped on the reactor while the other one was earthed. It was an inductively coupled system: the external electrode and the glass reactor wall underneath it, together with the conductive plasma inside the reactor, create a capacitor that enabled capacitive coupling of RF power into the discharge.[19]

A diffusion pump was used to keep the system pressure lower than 0.00075 mbar for the cleanup of contamination before the experiment. For each designed experimental condition, the input power, the O_2/CHF_3 or H_2/CHF_3 ratio, the operational pressure, and the CHF_3 feeding concentration were measured more than three times within 5 min to ensure steady-state conditions being achieved. The reactants and final products were identified by a gas chromatography/mass spectrometry (Varian Saturn 2000 GC/MS, GC column is DB-1, J&W scientific, 60 m × 0.32 mm) first and identified and quantified by an on-line Fourier transform infrared (FTIR) spectrometer (Bio-Rad, Model FTS-7).

The reactants and products were also sampled from the outlet valve on the downstream of the plasma reactor through a canister sampler (Figure 1). The collected gas was separately injected into the GC/MS and the GC-FID (gas chromatography-flame ionization detector) systems by a thermal desorption apparatus. Fluorocarbons were analyzed by the GC/MS, while hydrocarbons were analyzed by the GC-FID. Calibration of gaseous reactants and products was made by withdrawing unreacted gases and by going directly through the sampling line connected to the FTIR. The mass of species was calculated by comparing the response factor (absorbance height/concentration) of standard gas at the same IR wavenumber.[14,15,20] To understand the significance of deposition and condensation that occurred in the sampling and analyzing system, the FTIR quantification data were also checked through a carbon balance.

Each run of experiments lasted for 20 min and the results showed that the steady-state conditions were approached in the effluent after 10 min. The data reported herein are based on the mean values measured after a steady-state condition being reached. Each run of the effluent concentration of individual species were monitored by FTIR and confirmed by GC/MS.

2.2. Experimental Conditions. Experiments were conducted to determine the dependence of the CHF_3 decomposition fraction (η_{CHF_3}) and the fraction of total carbon input converted into CO_2 or $CH_4 + C_2H_2$ (F_{CO_2} and $F_{CH_4+C_2H_2}$) on various experimental parameters, including A_1 and A_2 for the input power, B_1 for the O_2/CHF_3 ratio and B_2 for the H_2/CHF_3 ratio, C_1 and C_2 for the operational pressure, and D_1 and D_2 for the CHF_3 feeding concentration. The subscripts 1 and 2 on the A, B, C, and D represent the $CHF_3/O_2/Ar$ system and the $CHF_3/H_2/Ar$ plasma system, respectively. Theη_{CHF_3}, F_{CO_2}, and $F_{CH_4+C_2H_2}$ were defined as follows:

$$\eta_{CHF_3}(\%) = [(C_{in} - C_{out})/(C_{in})] \times 100\% \qquad (1)$$

C_{in} is the feeding concentration of CHF_3 (%) and C_{out} is

Table 1. Designed and Operational Experimental Conditions

	designed conditions		operational conditions	
parameter	CHF_3/O_2/Ar	CHF_3/H_2/Ar	CHF_3/O_2/Ar	CHF_3/H_2/Ar
input power (W)	100	100	40−120	40−110
flow rate (sccm)				
Ar	80	80	0−90	0−90
CHF_3	10	10	5−20	5−20
O_2 or H_2	10	10	5−90	5−90
operational pressure (mbar)	11.3	11.3	7.5−18.8	7.5−18.8

the effluent concentration of CHF_3 (%).

$$F_{CO_2}(\%) = [C_{CO_2}/C_{in}] \times 100\% \quad (2)$$

C_{CO_2} is the effluent concentration of CO_2 (%).

$$F_{CH_4+C_2H_2}(\%) = [(C_{CH_4} + 2C_{C_2H_2})/(C_{in})] \times 100\% \quad (3)$$

C_{CH_4} is the effluent concentration of CH_4 (%) and $C_{C_2H_2}$ is the effluent concentration of C_2H_2 (%).

All experiments were conducted under the designed experimental parameters shown in Table 1. The global reactions of CHF_3 with O_2 and H_2, respectively, in the RF plasma system were as follows:

$$CHF_3 + O_2 = CO_2 + HF + F_2 \quad (4)$$

$$3CHF_3 + 6H_2 = CH_4 + C_2H_2 + 9HF \quad (5)$$

3. Methods of Analysis

The fractional factorial design method being proposed by Box et al.[21] was established to identify the key variables in influencing theη_{CHF_3}, F_{CO_2}, and $F_{CH_4+C_2H_2}$. The experimental results were subjected to regression analysis and generated the following equations:

$$\eta_{CHF_3} = 98.12 + 1.01A_1 - 0.47B_1 - 0.11C_1 - 0.45D_1 \quad (R^2 = 0.98) \quad (6)$$

$$F_{CO_2} = 86.28 + 2.67A_1 - 0.66B_1 - 0.37C_1 - 2.03D_1 \quad (R^2 = 0.96) \quad (7)$$

$$\eta_{CHF_3} = 48.09 + 25.13A_2 - 7.05B_2 - 0.16C_2 - 14.53D_2 \quad (R^2 = 0.96) \quad (8)$$

$$F_{CH_4+C_2H_2} = 33.60 + 17.39A_2 - 3.45B_2 - 2.28C_2 - 11.82D_2 \quad (R^2 = 0.97) \quad (9)$$

The aim of model sensitivity analysis was to gain better insight into the relative importance of the various experimental parameters for the RF plasma reactor. Estimates of the model sensitivity analysis were based on eqs 6−9 and followed the procedure recommended by Hsieh et al.[18] The sensitivity coefficient was defined as follows:

$$R_{ij} = (\Delta S/S)/(\Delta\lambda/\lambda) \quad (10)$$

R is the sensitivity coefficient forη_{CHF_3}, R' is the sensitivity coefficient for F_{CO_2} or $F_{CH_4+C_2H_2}$, i is the experimental parameter (A, B, C, or D), j is 1 for the CHF_3/O_2/Ar plasma system and 2 for CHF_3/H_2/Ar plasma system, $\Delta S/S$ are the changes (%) ofη_{CHF_3}, F_{CO_2}, or $F_{CH_4+C_2H_2}$ (%) for each experimental parameter (A, B, C, D) standardized by the initial predicted value, respectively, and $\Delta\lambda/\lambda$ is, for each experimental parameter (A, B, C, D), respectively, the amount increasing or decreasing divided by the initial value.

Table 2. Sensitivity Coefficients for the Decomposition Fraction of CHF_3 (η_{CHF_3})

	CHF_3/O_2/Ar	CHF_3/H_2/Ar
A: input power	$R_{A_1} = 0.010$	$R_{A_2} = 0.523$
B_1: O_2/CHF_3 ratio	$R_{B_1} = -0.005$	$R_{B_2} = -0.147$
B_2: H_2/CHF_3 ratio		
C: operational pressure	$R_{C_1} = -0.001$	$R_{C_2} = -0.003$
D: CHF_3 feeding concentration	$R_{D_1} = -0.005$	$R_{D_2} = -0.302$

Table 3. Sensitivity Coefficients for the Total Carbon Input Converted into CO_2 or $CH_4 + C_2H_2$ (F_{CO_2} or $F_{CH_4+C_2H_2}$)

	CHF_3/O_2/Ar (F_{CO_2})	CHF_3/H_2/Ar ($F_{CH_4+C_2H_2}$)
A: input power	$R'_{A_1} = 0.031$	$R'_{A_2} = 0.518$
B_1: O_2/CHF_3 ratio	$R'_{B_1} = -0.008$	$R'_{B_2} = -0.103$
B_2: H_2/CHF_3 ratio		
C: operational pressure	$R'_{C_1} = -0.004$	$R'_{C_2} = -0.068$
D: CHF_3 feeding concentration	$R'_{D_1} = -0.024$	$R'_{D_2} = -0.352$

4. Results of Measurements

4.1. Model Sensitivity Analysis. The results of model sensitivity analysis were given in Figure 2. The steeper the straight line, the greater the absolute magnitude of the sensitivity coefficient, and the more influence it will have on the experimental parameter. The absolute magnitude of the sensitivity coefficient forη_{CHF_3} in the CHF_3/O_2/Ar plasma system was $|R_{A_1}| > |R_{B_1}| > |R_{D_1}| > |R_{C_1}|$ and that in the CHF_3/H_2/Ar plasma system was $|R_{A_2}| > |R_{D_2}| > |R_{B_2}| > |R_{C_2}|$ (Table 2). The input power was the most influential parameter and only it exhibits a positive effect in both plasma systems.

The absolute magnitude of R' for F_{CO_2} in the CHF_3/O_2/Ar system was $|R'_{A_1}| > |R'_{D_1}| > |R'_{B_1}| > |R'_{C_1}|$ and that for $F_{CH_4+C_2H_2}$ in the CHF_3/H_2/Ar system was $|R'_{A_2}| > |R'_{D_2}| > |R'_{B_2}| > |R'_{C_2}|$ (Table 3). The input power and CHF_3 feeding concentration were the two most influential parameters in both plasma systems. Only parameter A exhibits a positive impact, while B, C, and D have a negative effect. In addition, the R'_2 was approximately 12.9−17.0 times of magnitude higher than R'_1. The following results and discussion were focused on the influence of parameter A and B.

4.2. Deposition. There was apparently white film deposition formed on the inside and downstream of the plasma reactor both in the CHF_3/O_2/Ar and CHF_3/H_2/Ar plasma systems. The result of chemical analysis (ESCA, ESCA-210) by using electron spectroscopy for the elemental contents of this white film deposition on the inner wall and downstream of the RF plasma reactor showed that there was carbon, fluorine, oxygen, and silicon involved in the CHF_3/O_2/Ar RF plasma system, while there was carbon, fluorine, and silicon involved in the CHF_3/H_2/Ar RF plasma system. Film formation was possibly because of the unsaturated fluorocarbon radicals presented and oligomers derived from the feed gas as precursors to inhibitor sidewall protection films.[22] The addition of oxygen will increase the etchant concentrations or suppress the polymer. However, hydrogen

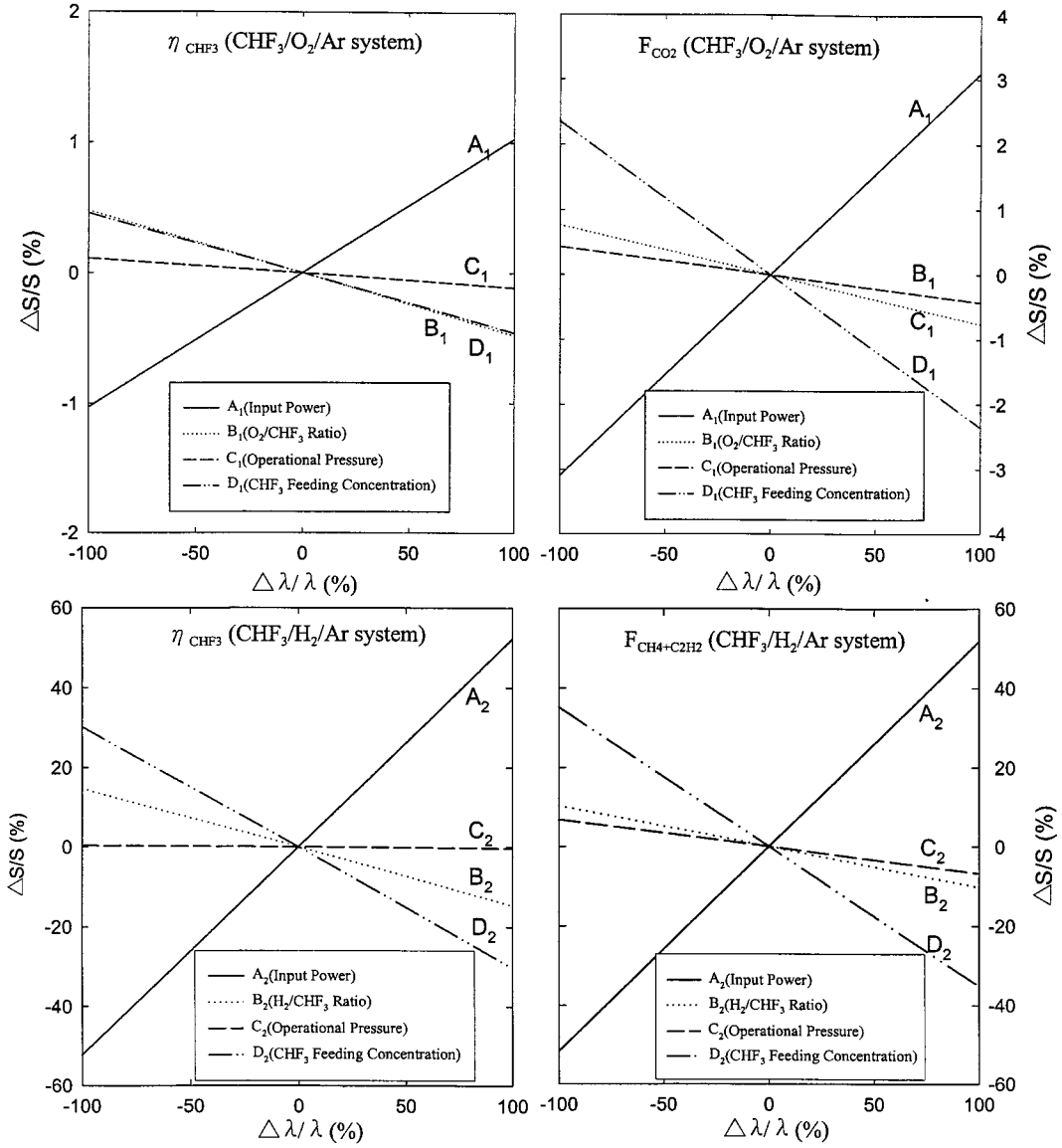

Figure 2. Model sensitivity analysis for η_{CHF_3}, F_{CO_2}, and $F_{CH_4+C_2H_2}$ in the CHF_3/O_2/AR and CHF_3/H_2/Ar systems, respectively.

added to fluorocarbon feeds will promote CF_x film growth for selective SiO_2 etching.[22] Furthermore, the polymerization process with the addition of H_2 to the Ar plasma propagates the polymerization chiefly by a radical mechanism.[23] The results of photographs of deposition peeling off downstream of the plasma reactor for scanning electron microscopy (SEM, JXA840A) with oxygen or hydrogen addition showed that the smaller and denser crystals were formed with hydrogen input (Figure 3).

4.3. CHF_3 Decomposition Fraction. Carbon balance and η_{CHF_3} with various input powers were shown in Figure 4. In both the CHF_3/O_2/Ar and CHF_3/H_2/Ar plasma systems, the carbon balance decreased and η_{CHF_3} increased by increasing the input power. In the CHF_3/O_2/Ar plasma system, the η_{CHF_3} was 99.6% when the input power was 60 W, while in the CHF_3/H_2/Ar plasma system, the η_{CHF_3} was only 55.0% at the same input power.

Figure 5 showed both carbon balance and η_{CHF_3} in the CHF_3/O_2/Ar and the CHF_3/H_2/Ar plasma system, respectively under various O_2/CHF_3 (B_1) or H_2/CHF_3 (B_2) ratios. All the values of carbon balance are between 0.90 and 0.99 (Figure 5A). In addition, the η_{CHF_3} was near 100% when the B_1 was between 0.5 and 1.0 and slowly decreased to 95.4% at 9.0 of B_1. Interestingly, the η_{CHF_3} was 99.6% when the B_2 was 0.5 and sharply decreased to 32.6% at 9.0 of B_2.

4.4. Detected Products. The same species detected in the effluent gas streams of both the CHF_3/O_2/Ar and CHF_3/H_2/Ar plasma systems were CHF_3, CH_2F_2, CF_4, HF, and SiF_4. However, the CO_2 and COF_2 were only detected in those of the CHF_3/O_2/Ar plasma system and the CH_4, C_2H_2, and CH_3F were only detected in those of the CHF_3/H_2/Ar plasma system. The formation of SiF_4 was due to the well-known plasma-chemical etching reaction shown as follows:

$$^{23}CF_4 + SiO_2 = SiF_4 + CO_2 \qquad (11)$$

$$^{22}4F + SiO_2 = SiF_4 + O_2 \qquad (12)$$

In the effluent gas stream, SiF_4 can be converted into CaF_2 and be removed according to the research of Breitbarth.[20]

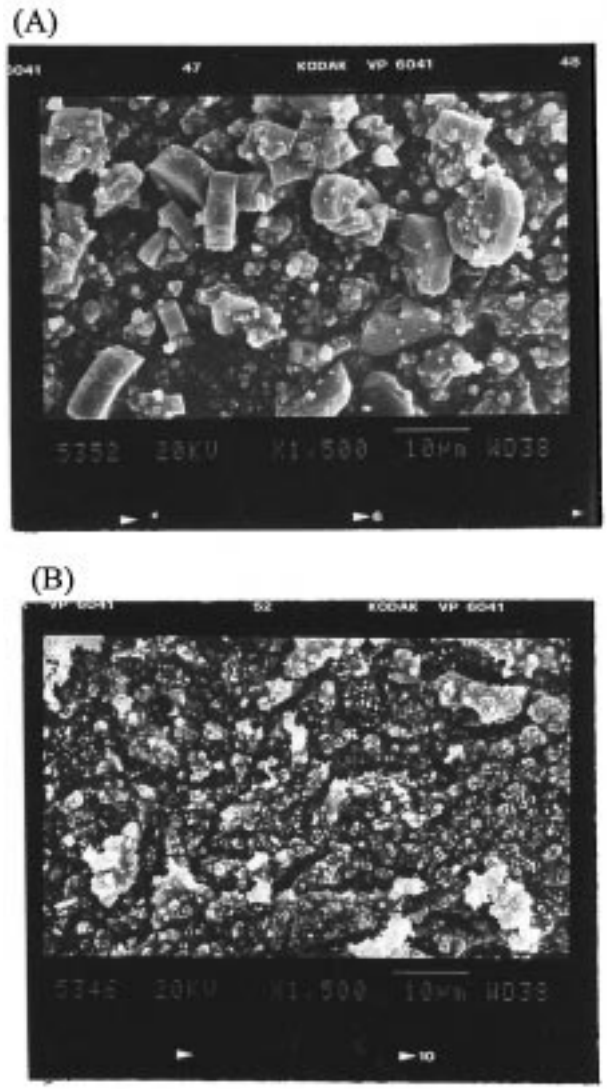

Figure 3. (a) Deposition in the CHF_3/O_2/Ar plasma system; (b) deposition in the CHF_3/H_2/Ar plasma system.

Figure 6 showed the F_{CO_2} in the effluent stream of the CHF_3/O_2/Ar plasma system and the F_{CH_4} and $F_{C_2H_2}$ in that of the CHF_3/H_2/Ar plasma system under various input powers. CO_2 was the most dominant carbonaceous final product in the CHF_3/O_2/Ar plasma system and F_{CO_2} increased moderately from 86.0% to 90.5% with the increasing input power (Figure 6A). The F_{CH_4} and $F_{C_2H_2}$ in the CHF_3/H_2/Ar plasma system increased from 9.69% to 33.0% and from 8.69% to 51.1%, respectively (Figure 6B).

The mole fractions of HF (M_{HF}) increased slowly from 38.3% to 39.0% in the CHF_3/O_2/Ar plasma system, while those in the CHF_3/H_2/Ar plasma increased sharply from 29.7% to 63.7% (Figure 7). In addition, the mole fraction of SiF_4 (M_{SiF_4}) in the CHF_3/O_2/Ar plasma system was higher than that in the CHF_3/H_2/Ar plasma system (Figure 8).

Figure 9 showed the mole fraction of COF_2 (M_{COF_2}) in the CHF_3/O_2/Ar plasma system, the mole fraction of CH_3F (M_{CH_3F}) in the CHF_3/H_2/Ar plasma system, and the mole fractions of CH_2F_2 ($M_{CH_2F_2}$) and CF_4 (M_{CF_4}) in both systems. When the input power was from 40 to 120 W, the M_{COF_2} ranged between 0.57% and 0.01% (Figure 9A). In addition, the mean values of $M_{CH_2F_2}$ and M_{CF_4} were 2.04% and 0.64%, respectively (Figure 9B). Figure

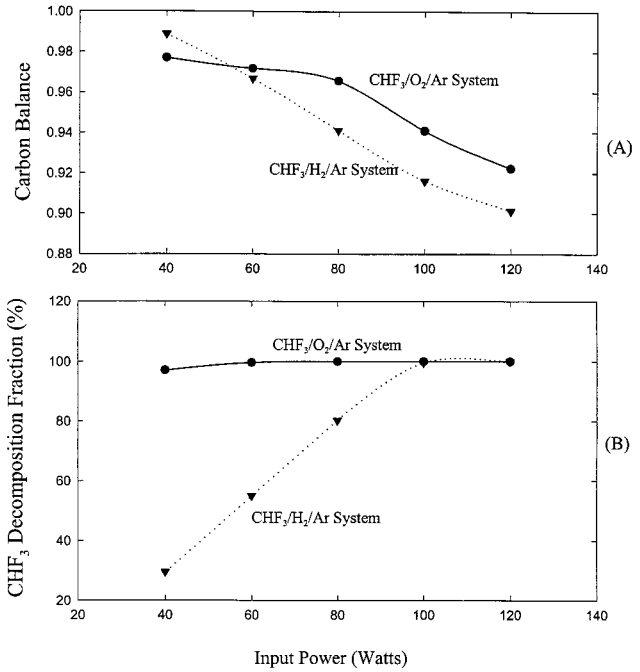

Figure 4. Carbon balance and CHF_3 decomposition fraction under various input powers in the CHF_3/O_2/Ar and CHF_3/H_2/Ar systems, respectively. ($O_2/CHF_3 = 1.0$, $H_2/CHF_3 = 1.0$, operational pressure = 11.3 mbar, CHF_3 feeding concentration = 10%).

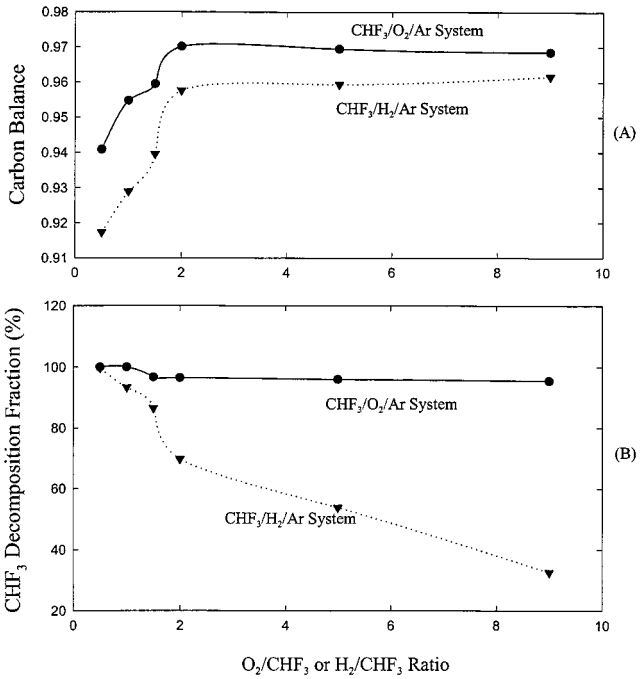

Figure 5. Carbon balance and CHF_3 decomposition fraction under various O_2/CHF_3 or H_2/CHF_3 ratios in the CHF_3/O_2/Ar and CHF_3/H_2/Ar system, respectively (input power = 100 W, operational pressure = 11.3 mbar, CHF_3 feeding concentration = 10%).

9C showed that the mean values of $M_{CH_2F_2}$, M_{CH_3F}, and M_{CF_4} were 1.77%, 1.34%, and 0.82%, respectively.

Figure 10 showed the F_{CO_2} in the CHF_3/O_2/Ar plasma system and F_{CH_4} and $F_{C_2H_2}$ in the CHF_3/H_2/Ar plasma system under various O_2/CHF_3 (B_1) or H_2/CHF_3 (B_2) ratios. There was no argon involved when the B_1 or B_2 was at 9.0. The F_{CO_2} increased slightly from 87.9% to 89.5% with the B_1 increasing from 0.5 to 1.0, but itdecreased from 89.5% to 86.0% with the B_1 increasing from 1.0 to 9.0 (Figure 10A). The distribution of F_{CH_4}

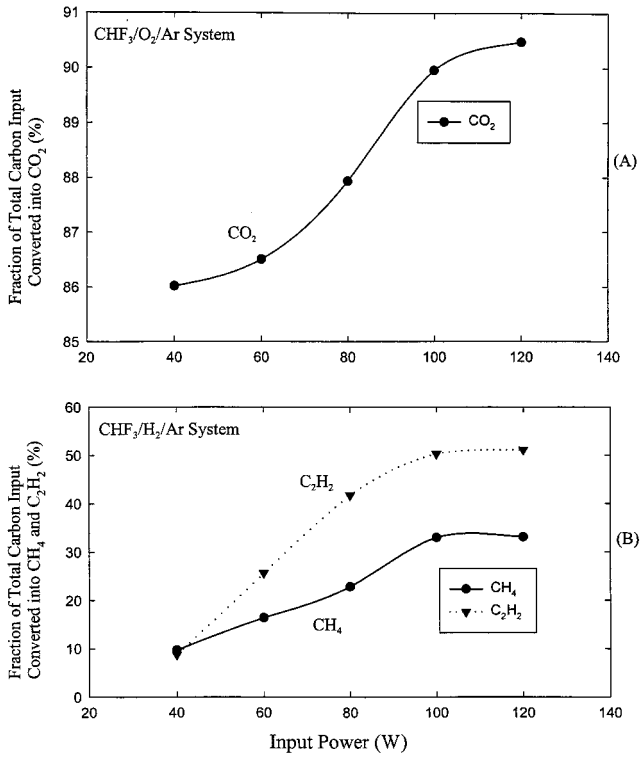

Figure 6. Fraction of total carbon input converted into CO_2 in the $CHF_3/O_2/Ar$ system and that of CH_4 and C_2H_2 in the $CHF_3/H_2/Ar$ system under various input powers ($O_2/CHF_3 = 1.0$, $H_2/CHF_3 = 1.0$, operational pressure = 11.3 mbar, CHF_3 feeding concentration = 10%).

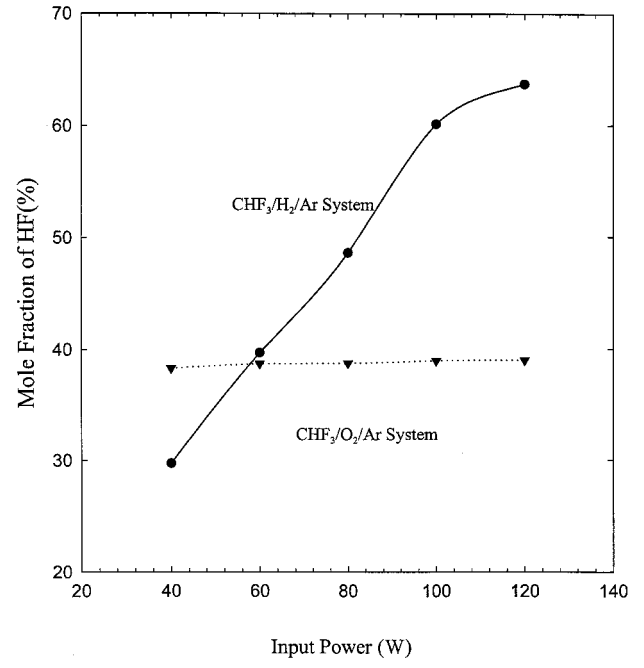

Figure 7. Mole fraction of HF in the effluent gas stream of the $CHF_3/O_2/Ar$ system and that of the $CHF_3/H_2/Ar$ system under various input powers ($O_2/CHF_3 = 1.0$, $H_2/CHF_3 = 1.0$, operational pressure = 11.3 mbar, CHF_3 feeding concentration = 10%).

was the same as that of F_{CO_2}, increasing from 26.2% to 36.0% with B_2 from 0.5 to 1.0 and decreasing to 21.3% with B_2 at 9.0. Furthermore, the $F_{C_2H_2}$ decreased apparently from 56.2% to 4.44% at B_2 from 0.5 to 9.0 (Figure 10B).

The F_{HF} decreased slightly from 39.2% to 37.5% with B_1 from 0.5 to 9.0 in the $CHF_3/O_2/Ar$ plasma system,

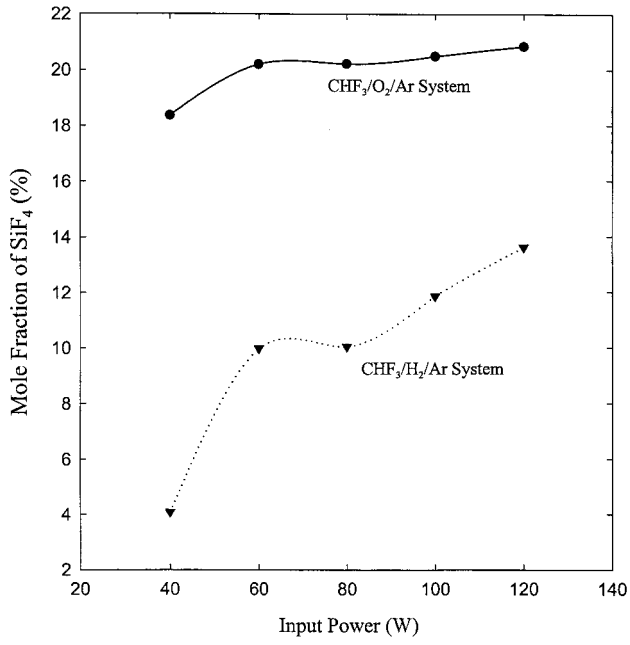

Figure 8. Mole fraction of SiF_4 in the effluent gas stream of $CHF_3/O_2/Ar$ and that of the $CHF_3/H_2/Ar$ system, respectively, under various input powers ($O_2/CHF_3 = 1.0$, $H_2/CHF_3 = 1.0$, operational pressure = 11.3 mbar, CHF_3 feeding concentration = 10%).

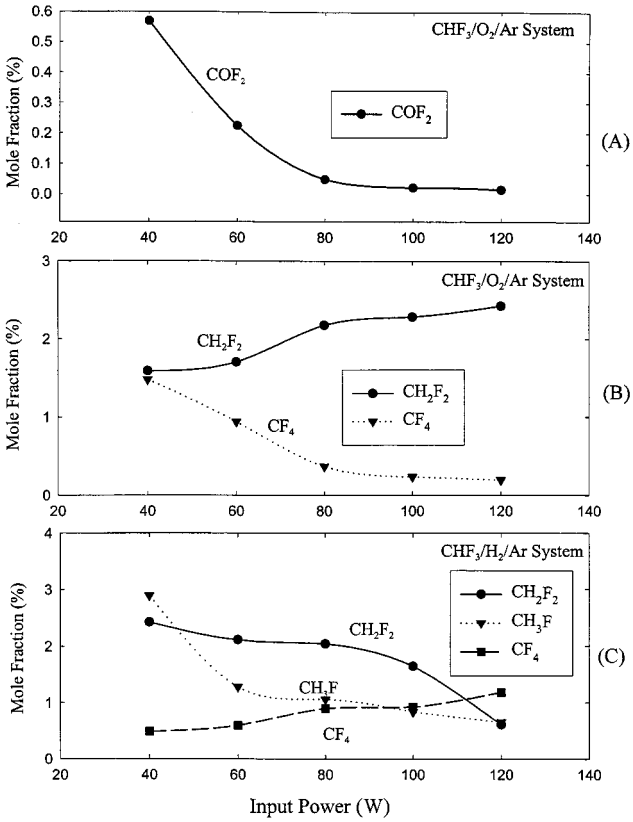

Figure 9. Mole fraction of COF_2, CH_2F_2, and CF_4 in the effluent gas stream of the $CHF_3/O_2/Ar$ system and mole fraction of CH_2F_2, CH_3F, and CF_4 in that of the $CHF_3/H_2/Ar$ system under various input powers ($O_2/CHF_3 = 1.0$, $H_2/CHF_3 = 1.0$, operational pressure = 11.3 mbar, CHF_3 feeding concentration = 10%).

while it increased from 54.8% to 63.4% with B_2 from 0.5 to 1.5 but decreased to 42.5% at a B_2 of 9.0 in the $CHF_3/H_2/Ar$ plasma system (Figure 11).

Figure 12 showed the M_{SiF_4} in the $CHF_3/O_2/Ar$ and $CHF_3/H_2/Ar$ plasma systems. M_{SiF_4} increased from 20.1%

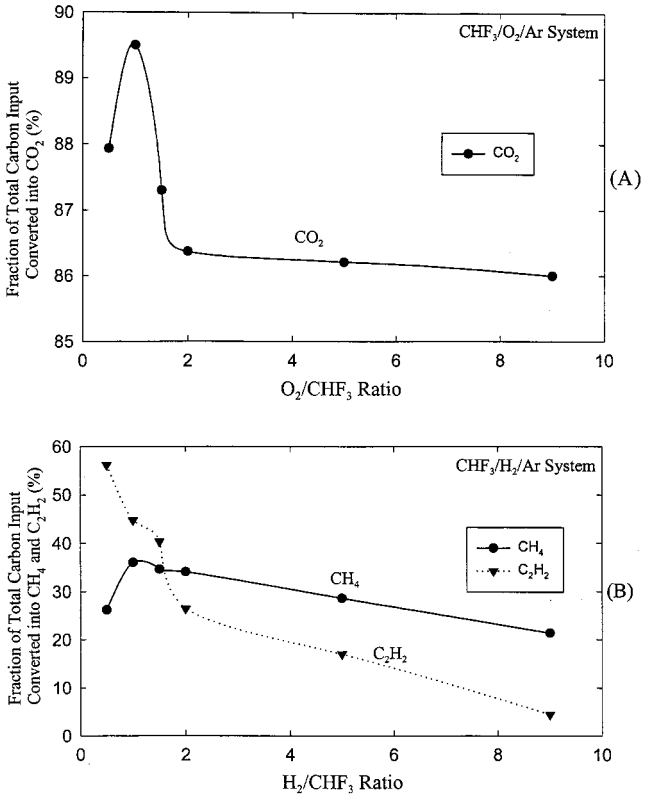

Figure 10. Fraction of total carbon input converted into CO_2 in the $CHF_3/O_2/Ar$ system and that of CH_4 and C_2H_2 in the $CHF_3/H_2/Ar$ system under various O_2/CHF_3 or H_2/CHF_3 ratios (input power = 100 W, operational pressure = 11.3 mbar, CHF_3 feeding concentration = 10%).

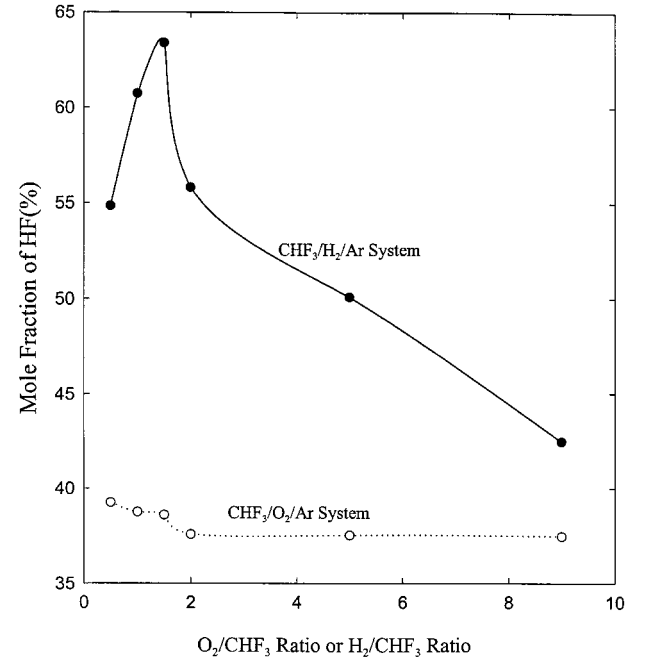

Figure 11. Mole fraction of HF in the effluent gas stream of the $CHF_3/O_2/Ar$ system and that of the $CHF_3/H_2/Ar$ system under various O_2/CHF_3 or H_2/CHF_3 ratios (input power = 100 W, operational pressure = 11.3 mbar, CHF_3 feeding concentration = 10%).

to 20.6% with the B_1 increasing from 0.5 to 1.5, but decreased from 20.6% to 17.6% with B_1 increasing from 1.5 to 9.0. In the $CHF_3/H_2/Ar$ plasma system, M_{SiF_4} decreased sharply from 15.8% to 0.89% with the B_2 increasing from 0.5 to 9.0.

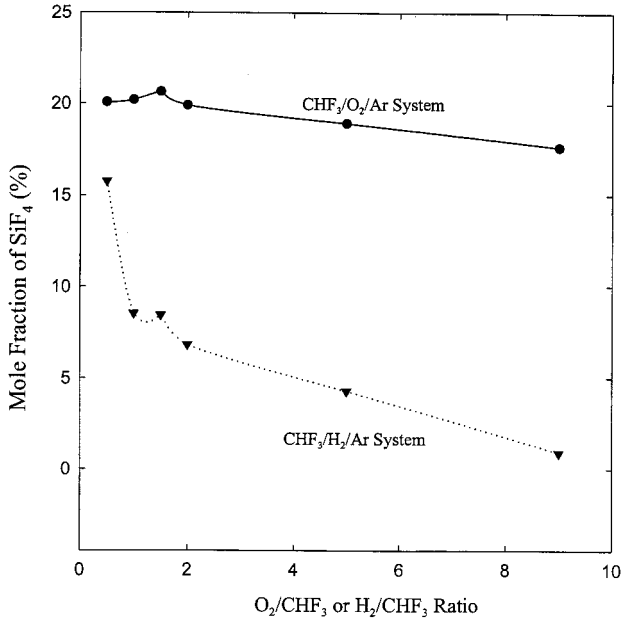

Figure 12. Mole fraction of SiF_4 in the effluent gas stream of $CHF_3/O_2/Ar$ and that of the $CHF_3/H_2/Ar$ system, respectively, under various O_2/CHF_3 or H_2/CHF_3 ratios (input power = 100 W, operational pressure = 11.3 mbar, CHF_3 feeding concentration = 10%).

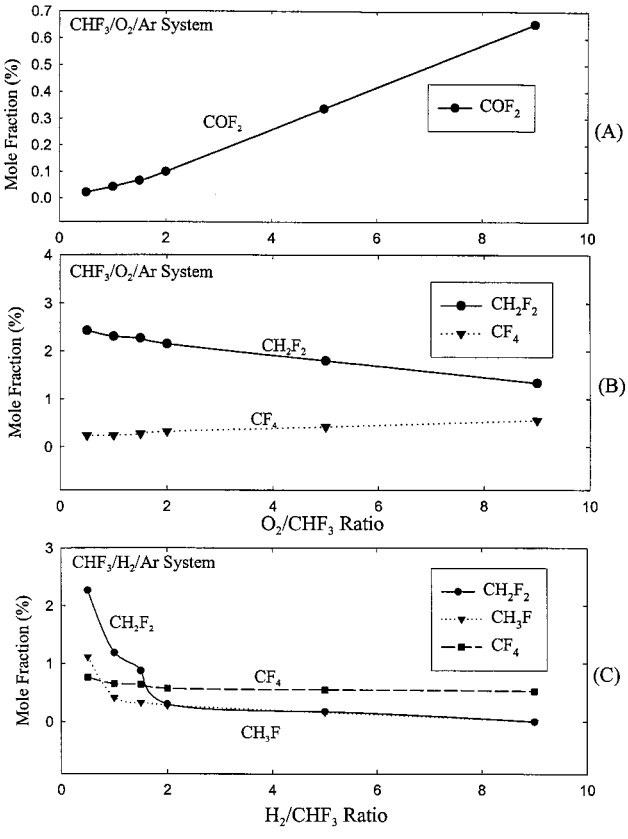

Figure 13. Mole fraction of COF_2, CH_2F_2, and CF_4 in the effluent gas stream of the $CHF_3/O_2/Ar$ system and mole fraction of CH_2F_2, CH_3F, and CF_4 in that of the $CHF_3/H_2/Ar$ system under various O_2/CHF_3 or H_2/CHF_3 ratios (input power = 100 W, operational pressure = 11.3 mbar, CHF_3 feeding concentration = 10%).

Figure 13 showed the M_{COF_2} in the $CHF_3/O_2/Ar$ plasma system, the M_{CH_3F} in the $CHF_3/H_2/Ar$ plasma system, and the $M_{CH_2F_2}$ and M_{CF_4} in both the $CHF_3/O_2/Ar$ and $CHF_3/H_2/Ar$ plasma system, respectively. The

M_{COF_2} increased from 0.02% to 0.65% when the O_2/CHF_3 ratio increased from 0.5 to 9.0 (Figure 13A). In addition, $M_{CH_2F_2}$ decreased from 2.43% to 1.33% and the M_{CF_4} increased from 0.24% to 0.55% as B_1 increased from 0.5 to 9.0 (Figure 13B). In the CHF_3/H_2/Ar plasma system, the $M_{CH_2F_2}$, M_{CH_3F}, and M_{CF_4} decreased from 2.26% to ≒0%, 1.11% to ≒0%, and 0.76% to 0.52%, respectively, when the B_2 increased from 0.5 to 9.0 (Figure 13C).

In comparison with the research of Yamamoto,[24] the decomposition efficiency of CHF_3 was much higher than that of CFC-113. Furthermore, the byproducts were much fewer and simpler in this study.

5. Discussion of Measured Data

5.1. The Possible Reaction Mechanism. Electrons, primarily generated by partial ionization of the molecules and atoms in RF plasma, are the principal sources for transferring electrical energy to the gas and initiate the chemical reactions.[13,23] In most reactions, molecules are first excited through direct collisions, via negative ions, or by recombination of positive ion with electrons. The excited molecules can be fragmented, or they can be isomerized to form either stable compounds or reactive intermediates.[23,25]

The initial reactions at the plasma system were excitation for Ar, which were similar in both the CHF_3/O_2/Ar and CHF_3/H_2/Ar plasma systems. These reactions were shown as follows:

$$^{23}Ar + e^- = Ar^* + e^- \quad (13)$$

$$^{23}Ar + e^- = Ar^+ + 2e^- \quad (14)$$

The superscripts represent the literature cited. In the CHF_3/O_2/Ar RF plasma reactor, the O_2 was dissociated and excited first. These reactions were shown as follows:

$$^{23}O_2 + e^- = O_2^* + e^- = O_2 + h\nu + e^- \quad (15)$$

$$^{23}O_2 + e^- = O_2^+ + 2e^- \quad (16)$$

$$^{23}O_2 + e^- = O_2^- \quad (17)$$

In addition, the M represents the third molecules. Similarly, in the CHF_3/H_2/Ar RF plasma reactor, H_2 was also dissociated and excited first. These reactions were shown as follows

$$^{23}H_2 + e^- = 2H + e^- \quad (18)$$

$$^{23}H_2 + e^- = H_2^* + e^- = H_2 + h\nu + e^- \quad (19)$$

$$^{23}H_2 + e^- = H + H^+ + 2e^- \quad (20)$$

$$^{26}H_2 + M = H + H + M \quad (21)$$

The results of the experiments showed that the highly electronegative fluorine[30] or the stable HF would easily separate from the CHF_3 molecule.

$$^{28}CHF_3 + (M, e^-) = CF_2 + HF + (M, e^-) \quad (22)$$

$$^{29}CHF_3 + F + M = CF_3 + HF + M \quad (23)$$

$$CHF_3 + (M, e^-) = CHF_2 + F + (M, e^-) \quad (24)$$

$$CHF_3 + O = (CF_3 + OH, CHF_2 + FO) \quad (25)$$

$$^{28}CHF_3 + H = (CHF_2 + HF, CF_3 + H_2) \quad (26)$$

Further elimination of these radicals gave the opportunities for reaction with the reacted gas (O_2 or H_2) and terminated the reactions to form CO_2, CH_4, or C_2H_2.

$$^{28}CHF_2 + (F, e^-) = (CF_2, CF + e^-) + HF \quad (27)$$

$$CHF_2 + (M, e^-) = CHF + F + (M, e^-) \quad (28)$$

$$CF_3 + (Ar^*, e^-) = CF_2 + F + (Ar, e^-) \quad (29)$$

$$^{26}CF_2 + M = CF + F + M \quad (30)$$

$$^{28}CHF_2 + H = (CF_2 + H_2, CHF + HF) \quad (31)$$

In the CHF_3/O_2/Ar plasma system, the main reaction pathway is the formation of CO_2, HF, and SiF_4. The high bond strength of OC═O (532.2 ± 0.4 D^0_{298}/kJ mol^{-1}) [27] on CO_2 might reduce the opportunities to produce other carbonaceous compounds. Furthermore, the high bond strength of H−F (567.9 ± 0.1 D^0_{298}/kJ mol^{-1}) and Si−F (552.7 ± 2.1 D^0_{298}/kJ mol^{-1})[27] on SiF_4 will reduce the opportunities for reaction between F and C atoms to form other fluorinated compounds.

In the CHF_3/H_2/Ar plasma system, the main reaction pathway is the formation of HF, CH_4, and C_2H_2, owing to the strong bond energy of these compounds. Adding a higher amount of H_2 into the reactor will form a preferential pathway for the HF formations. HF is a thermodynamically stable diatomic species that will limit the production of other fluorinated hydrocarbons.

CO_2 Formation Mechanism

$$^{29}CFO + O_2 = CO_2 + F + O \quad (32)$$

$$^{29}CFO + O = CO_2 + F \quad (33)$$

$$^{29}CFO + OH = CO_2 + HF \quad (34)$$

$$CF + 2O = CO_2 + F \quad (35)$$

$$CHF + 2O = CO_2 + HF \quad (36)$$

COF_2 Formation and Decomposition Mechanism

$$CHF_2 + O = COF_2 + H \quad (37)$$

$$^{28}CF_2 + (OH, O_2) = COF_2 + (H, O) \quad (38)$$

$$^{26}COF_2 + (O, M) = COF + (FO, F + M) \quad (39)$$

CH_4 Formation and Decomposition Mechanism

In the CHF_3/H_2/Ar plasma system, the formations of CH_4 and C_2H_2 were due to the CHF_3's decomposing into $CHF_2^\bullet$ by electron or third-molecule collision. Accordingly, consecutive addition of hydrogen was occurred to form CH_4. Furthermore, the various hydrocarbon radicals would combine with each other to form C_2H_2.

$$^{28}CH_3 + (CHF_2, CH_2F) = CH_4 + (CF_2, CHF) \quad (40)$$

$$^{28}CH_3 + (CH_3F, CH_2F_2) = CH_4 + (CH_2F, CHF_2) \quad (41)$$

$$CHF_2 + M + (CH_2, CH_3) = (CH_3, CH_4) + CF_2 + M \quad (42)$$

$$H_2 + M + (CHF_2, CH_2F) = (CH_2F, CH_3) + HF + M \quad (43)$$

$$^{18}CH_4 + (Ar^*, e^-) = CH_3 + H + (Ar, e^-) \quad (44)$$

$$^{18}CH_3 + (Ar^*, e^-) = CH_2 + H + (Ar, e^-) \quad (45)$$

$$^{18}CH_2 + (Ar^*, e^-) = CH + H + (Ar, e^-) \quad (46)$$

C_2H_2 Formation and Decomposition Mechanism

$$CH_2 + CH_2 = C_2H_4 \quad (47)$$

$$C_2H_4 + H = C_2H_3 + H_2 \quad (48)$$

$$C_2H_3 + H = C_2H_2 + H_2 \quad (49)$$

$$^{18}CH + (CH_2, CH) = C_2H_2 + H \quad (50)$$

High production of CH_xF_y and CF_x radicals led to the production of other fluorinated compounds.

HF Formation and Decomposition Mechanism

$$^{28}F + (CH_2F_2, CH_2F) = HF + (CHF_2, CHF) \quad (51)$$

$$^{26}H + F_2 = HF + F \quad (52)$$

$$^{28}H_2 + F = HF + H \quad (53)$$

$$^{28}CH_3F = HF + CH_2 \quad (54)$$

$$^{28}CH_3F + (M, H) = HF + (CF_2 + M, CH_3) \quad (55)$$

$$CH_2F + (H, e^-) + M = (HF, F + e^-) + CH_2 + M \quad (56)$$

$$(C_2H_4, C_2H_3) + F = HF + (C_2H_3, C_2H_2) \quad (57)$$

$$^{28}HF + M = H + F + M \quad (58)$$

CH_2F_2 Formation and Decomposition Mechanism

$$^{28}CHF_2 + (CHF_2, CH_2F) = CH_2F_2 + (CF_2, CHF) \quad (59)$$

$$^{28}CHF + HF = CH_2F_2 \quad (60)$$

$$^{28}CF_2 + H_2 = CH_2F_2 \quad (61)$$

$$^{28}CHF_2 + H = (CH_2F_2, CHF + HF) \quad (62)$$

$$^{28}CH_2F_2 + F = CHF_2 + HF \quad (63)$$

$$^{28}CH_2F_2 + H = (CHF_2 + H_2, CH_2F + HF) \quad (64)$$

CF_4 Formation and Decomposition Mechanism

$$^{28}CF_3 + F = CF_4 \quad (65)$$

$$CF_2 + 2F = CF_4 \quad (66)$$

$$CF_2 + (Ar^*, e^-) = CF + F + (Ar, e^-) \quad (67)$$

$$^{28}CF + F = CF_2 \quad (68)$$

$$O + (CF_4, CF_3) = FO + (CF_3, CF_2) \quad (69)$$

$$^{28}H + (CF_4, CF_3, CF_2) = HF + (CF_3, CF_2, CF) \quad (70)$$

CH_3F Formation and Decomposition Mechanism

$$^{28}CHF + H_2 = CH_3F \quad (71)$$

$$^{28}CH_2F + H = CH_3F \quad (72)$$

$$^{28}CH_2F + (CH_2F, CHF_2) = CH_3F + (CHF, CF_2) \quad (73)$$

$$^{28}CH_3F + (CH_3, C_2H_3) = CH_2F + (CH_4, C_2H_4) \quad (74)$$

The CHF_3 will be regenerated as follows.

$$^{28}CF_3 + H_2 = CHF_3 + H \quad (75)$$

$$^{28}CF_3 + CH_4 = CHF_3 + CH_3 \quad (76)$$

$$^{28}CH_3F + CF_3 = CHF_3 + CH_2F \quad (77)$$

$$^{28}CH_2F_2 + CF_3 = CHF_3 + CHF_2 \quad (78)$$

The flow diagrams of possible reaction pathways for decomposition of CHF_3 in the $CHF_3/O_2/Ar$ and $CHF_3/H_2/Ar$ plasma systems were shown in Figures 14 and Figure 15, respectively.

5.2. The Effect of Deposition. Deposition formation will lead to the decrease of carbon balance. At higher input power, more polymerization was found in the plasma reactor, which resulted in a lower carbon balance in the effluent gas stream (Figures 4A and 5A). Furthermore, the carbon balance in the $CHF_3/O_2/Ar$ plasma system was higher than that in the $CHF_3/H_2/Ar$ plasma system (except at 40 W), owing to the addition of oxygen, which will suppress the polymer.

5.3. The Effect of Input Power. Sustaining an RF plasma environment needs energy to produce the required ionization. The degree of ionization depends mostly on how much energy is input.[30] Hence, the input power was the more important experimental parameter in the RF plasma system. Higher input power along with higher temperature will shift the Maxwell−Boltzmann velocity distribution to a higher speeds which displayed higher energies.[31] This was why the η_{CHF_3} in Figure 4B increased with the increasing input power.

The reaction of oxygen with CH_xF_y radicals will form COF_2 (eqs 37 and 38) or CO_2 (eqs 32−36), which was more difficult to recombine with the F atom to form the CHF_3 (eqs 75−78). Comparatively, the reaction of hydrogen with CHF_3 will easily form the thermodynamically stable HF and there were more opportunities for the rest of CH_xF_y radicals to recombine with each other or the F atom to form CHF_3 (eqs 75−78). This was possibly why the η_{CHF_3} in the $CHF_3/O_2/Ar$ plasma system was much higher than that in the $CHF_3/H_2/Ar$ plasma system when the input power was lower than 100 W. However, the effective collision frequencies increased

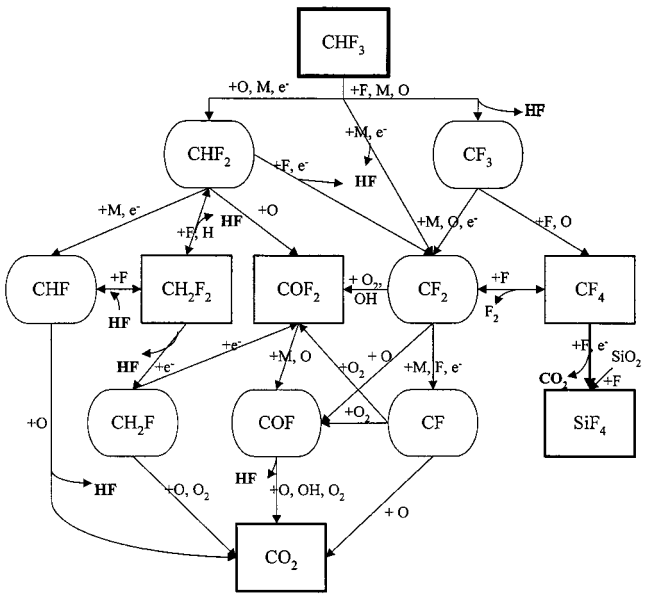

Figure 14. Flow diagram of possible reaction pathways for the decomposition of CHF_3 in the CHF_3/O_2/Ar RF plasma system.

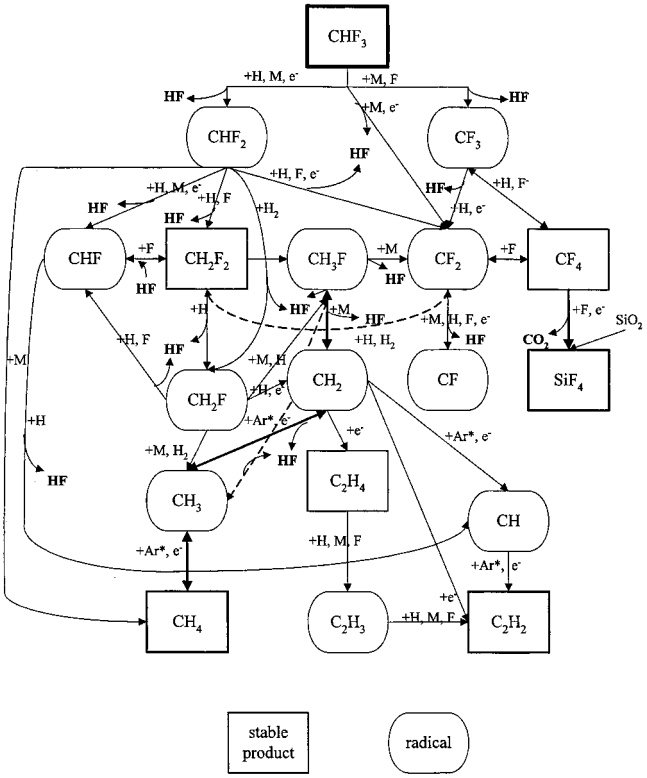

Figure 15. Flow diagram of possible reaction pathways for the decomposition of CHF_3 in the CHF_3/H_2/Ar RF plasma system.

while the input power was increasing. The higher collisional frequencies with input power higher than 100 W probably increased the reaction rate of eqs 22−26 and formed a new balance of CHF_3 decomposing and recombining.

A higher input power provided more energy and more opportunities for effective collision in the reactor and resulted in a higher reaction rate; it then created more opportunities for the reactants to be converted into CO_2 (eqs 32−36), CH_4 (eqs 40−42), and C_2H_2 (eqs 49 and 50) (Figure 6).

The etching reaction rate constant was proportional to the magnitude of plasma power input due to the etch process being plasma-activated.[20] Interestingly, the M_{SiF_4} was much higher in the CHF_3/O_2/Ar plasma system than that in the CHF_3/H_2/Ar plasma system (Figure 8). This was due to the hydrogen combining with F atoms to produce a very high amount of HF in the CHF_3/H_2/Ar plasma system (Figure 7). The reverse reaction of HF was difficult to proceed because of the high stability of HF. By contrast, limited hydrogen led to limited HF formation in the CHF_3/O_2/Ar plasma system. This made the excess F radicals react rapidly with SiO_2 to produce SiF_4. Hence, the M_{SiF_4} was much higher in the CHF_3/O_2/Ar plasma system than that in the CHF_3/H_2/Ar plasma system.

In the CHF_3/O_2/Ar plasma system, most of the input carbon atoms were transformed into CO_2, while a few of the carbons were converted into CH_2F_2, CF_4, and COF_2. The stronger bond of H−F on HF and Si−F on SiF_4,[27] respectively, made F radicals or ions easily to combine with H or SiF_x radicals to form a very significant amount of HF and SiF_4 (Figures 7 and 8) and a minor amount of CH_2F_2, CF_4, and COF_2 (Figure 9A,B). Figures 7−9 revealed that a higher input power promoted greater amounts of F atoms to form SiF_4 and hindered the possibility of COF_2 formation. The results indicated there will be more CHF_2 and CH_2F radicals produced to form CH_2F_2, owing to the increasing energy for decomposition of CHF_3 when the input power was increased. However, the CF_3 radical will compete with SiF_x and H radicals for the F radicals to form CF_4. Higher input power will provide higher opportunities for effective collision between molecules. It was easier for F radicals to form SiF_4 and HF, owing to the strong chemical bonds in Si−F and H−F. This all led to the downward trends of M_{CF_4} (Figure 9B).

In the CHF_3/H_2/Ar plasma system, it was obvious that the CHF_2 and CH_2F radicals were more dominant than the CF_x radicals at lower input power (Figure 9C). The stable HF formation made the rest of the CH_xF_y radicals to recombine with each other or H radicals to form CH_2F_2 (eqs 59−62) and CH_3F (eqs 71−73). But the increasing input power led to the CH_2F_2 and CH_3F decomposing.

5.4. The Effect of O_2/CHF_3 and H_2/CHF_3 Ratios. Figure 5B showed that adding more reacting molecules (H_2 or O_2) into the RF plasma system all lead to lower electron energy and then resulted in a lower η_{CHF_3}. However, the addition of hydrogen into the plasma reactor increased the recombination opportunities to form CHF_3 and apparently reduced the η_{CHF_3}, but the influence of added oxygen to the η_{CHF_3} was quite minor in the CHF_3/O_2/Ar plasma system in comparison to that in the hydrogen-based plasma system.

There will be more free fluorine produced at first[30] due to the reaction of oxygen with CH_xF_y radicals and then CO_2 and COF_2[22] will form (Figure 13A). However, if excess oxygen was added, the unsaturated compounds were depleted, owing to the limited reactants, and then it reduced the production of CO_2. CO_2 is a very stable compound which needs sufficient energy supply to form. Dilution of Ar concentration in the RF plasma reactor will reduce the transfer of energy and decrease the F_{CO_2}. Therefore, the F_{CO_2} increased between the $B_1 = 0.5$ and 1.0 and then decreased over $B_1 = 1.0$ (Figure 10A). In the CHF_3/H_2/Ar plasma system, a lower H_2/CHF_3 ratio along with a higher Ar concentration will increase the probability to convert the produced CH_4 into $CH_3^{\bullet}$, $CH_2^{\bullet}$, and $CH^{\bullet}$ and then formed a more stable C_2H_2,[18,32] owing

to a higher attacking ability of excited Ar*. Further on, the reduced energy transfer along with the higher B_2 resulted in the downward tendency of F_{CH_4} and $F_{C_2H_2}$.

A higher B_1 will decrease the Ar concentration in the CHF_3/O_2/Ar plasma system, reduce the efficiency of energy transfer, and then reduce the efficient collision opportunities for F radicals. On one hand, this was probably why the M_{HF} had downward trends with the increasing B_1. On the other hand, the M_{HF} increased with an increase of B_2 from 0.5 to 1.5 in the CHF_3/H_2/Ar plasma system (Figure 11). Adding excess hydrogen will cause a thin plasma polymer to coat on the surface until etching stops.[22] The thicker deposition on the surface of the reactor inhibited the etching process, reducing the SiF_4 production (Figure 12). The excess fluorine radicals or unsaturated fluorocarbons will follow eqs 51−57 to form HF. The limited reactants restricted the production of HF with the B_2 more than 1.5 and led to the decreasing of M_{HF} (Figure 11).

The addition of oxygen will increase the formation of COF_2 (eqs 37 and 38) which competed with SiO_2 to trap F radicals. Furthermore, the added oxygen will produce more free fluorine at first and then subsequently decrease because of dilution.[30] This was why the M_{SiF_4} increased at first and then decreased with the increasing B_1 (and Figure 12). A higher amount of H_2 addition will enhance the formation of stable HF and polymerization rather than etching.[19] This led to the decrease of SiF_4 as the B_2 increased.

In the CHF_3/O_2/Ar plasma system, increasing oxygen concentration will alter the balance between fluorine atoms and unsaturated compounds.[22]

$$^{22}(\text{O or } O_2) + CF_x = (COF_2 \text{ or } CO_2) + ((x-2)\text{F}, x\text{F}) \quad (79)$$

This will lead to a greater amount of COF_2 produced. The excess F• produced in eq 76 provided more opportunities for the CF_x• reacting with it to form CF_4 (eqs 65 and 66) and resulted in a slight increase in M_{CF_4}.

In the CHF_3/H_2/Ar plasma system, the formation of HF and limited reactants inhibited the production of other fluorinated hydrocarbons, CH_2F_2, CH_3F, and CF_4 with increasing of B_2.

6. Conclusions

CH_2F_2, CF_4, HF, and SiF_4 were detected in the effluent gas streams of both the CHF_3/O_2/Ar and CHF_3/H_2/Ar plasma systems. However, the CO_2 and COF_2 were detected only in the CHF_3/O_2/Ar plasma system gas stream and the CH_4, C_2H_2, and CH_3F were detected only in CHF_3/H_2/Ar plasma system gas stream.

The results of the model sensitivity analysis showed that the most sensitive coefficient for η_{CHF_3} in both the CHF_3/O_2/Ar and CHF_3/H_2/Ar plasma systems was the input power. A higher input power will lead to a higher η_{CHF_3} in both systems.

The results of the model sensitivity analysis also showed that the most sensitive parameter for F_{CO_2} in the CHF_3/O_2/Ar plasma system and $F_{CH_4+C_2H_2}$ in the CHF_3/H_2/Ar plasma system was also the input power. A higher input power will lead to a higher F_{CO_2} in the CHF_3/O_2/Ar plasma system and a higher $F_{CH_4+C_2H_2}$ in the CHF_3/H_2/Ar plasma system.

The M_{SiF_4} was much higher in the effluent gas stream of the CHF_3/O_2/Ar plasma system than that of the CHF_3/H_2/Ar plasma system. This was due to a higher amount of H_2 addition which will enhance the formation of stable HF and polymerization rather than etching. This will reduce the opportunities for the formation of SiF_4 in the CHF_3/H_2/Ar plasma system. In addition, excess hydrogen will cause a thin plasma polymer until the end of the etching process. Hence, fewer SiF_4 were produced.

The addition of hydrogen can produce a very significant amount of HF and inhibit the formation of SiF_4, CH_2F_2, CH_3F, and CF_4 and form useful CH_4 and C_2H_2. Even though the η_{CHF_3} in the CHF_3/H_2/Ar plasma system was lower than that in the CHF_3/O_2/Ar plasma system, but as a result of the greater advantages mentioned above, the hydrogen-based RF plasma system is a better alternative to decompose CHF_3.

Acknowledgment

The research was supported by funds from the National Science Council, Taiwan, Grant no. NSC 89-2211-E-006-012.

Notations

η_{CHF_3} = CHF_3 decomposition fraction (%)
C_{in} = feeding concentration of CHF_3 (%)
C_{out} = effluent concentration of CHF_3 (%)
F_{CO_2} = fraction of total carbon input converted into CO_2 (%)
C_{CO_2} = effluent concentration of CO_2 (%)
$F_{CH_4+C_2H_2}$ = fraction of total carbon input converted into CH_4 and C_2H_2 (%)
C_{CH_4} = effluent concentration of CH_4 (%)
$C_{C_2H_2}$ = effluent concentration of C_2H_2 (%)
R_{A_1} = sensitivity coefficient of the input power for η_{CHF_3} in the CHF_3/O_2/Ar plasma system
R_{A_2} = sensitivity coefficient of the input power for η_{CHF_3} in the CHF_3/H_2/Ar plasma system
R_{B_1} = sensitivity coefficient of the O_2/CHF_3 ratio for η_{CHF3} in the CHF_3/O_2/Ar plasma system
R_{B_2}= sensitivity coefficient of the H_2/CHF_3 ratio for η_{CHF_3} in the CHF_3/H_2/Ar plasma system
R_{C_1} = sensitivity coefficient of the operational pressure for η_{CHF_3} in the CHF_3/O_2/Ar plasma system
R_{C_2}= sensitivity coefficient of the operational pressure for η_{CHF_3} in the CHF_3/H_2/Ar plasma system
R_{D_1} = sensitivity coefficient of the CHF_3 feeding concentration for η_{CHF_3} in the CHF_3/O_2/Ar plasma system
R_{D_2} = sensitivity coefficient of the CHF_3 feeding concentration for η_{CHF_3} in the CHF_3/H_2/Ar plasma system
R'_{A_1} = sensitivity coefficient of the input power for F_{CO_2}
R'_{A_2} = sensitivity coefficient of the input power for $F_{CH_4+C_2H_2}$
R'_{B_1} = sensitivity coefficient of the O_2/CHF_3 ratio for F_{CO_2}
R'_{B_2} = sensitivity coefficient of the H_2/CHF_3 ratio for $F_{CH_4+C_2H_2}$
R'_{C_1} = sensitivity coefficient of the operational pressure for F_{CO_2}
R'_{C_2} = sensitivity coefficient of the operational pressure for $F_{CH_4+C_2H_2}$
R'_{D_1} = sensitivity coefficient of the CHF_3 feeding concentration for F_{CO_2}
R'_{D_2} = sensitivity coefficient of the CHF_3 feeding concentration for $F_{CH_4+C_2H_2}$
$\Delta S/S$ = the changes (%) of η_{CHF_3}, F_{CO_2}, or $F_{CH_4+C_2H_2}$ (%) for each experimental parameter standardized by the initial predicted value, respectively
$\Delta\lambda/\lambda$ = the amount of increase or reduction divided by the initial value for each experimental parameter, respectively

A_1 = experimental parameter for the input power (Watts) in the $CHF_3/O_2/Ar$ plasma system
A_2 = experimental parameter for the input power (Watts) in the $CHF_3/H_2/Ar$ plasma system
B_1 = experimental parameter for the O_2/CHF_3 ratio in the $CHF_3/O_2/Ar$ plasma system
B_2 = experimental parameter for the H_2/CHF_3 ratio in the $CHF_3/H_2/Ar$ plasma system
C_1 = experimental parameter for the operational pressure (mbar) in the $CHF_3/O_2/Ar$ plasma system
C_2 = experimental parameter for the operational pressure (mbar) in the $CHF_3/H_2/Ar$ plasma system
D_1 = experimental parameter for the CHF_3 feeding concentration (%) in the $CHF_3/O_2/Ar$ plasma system
D_2 = experimental parameter for the CHF_3 feeding concentration (%) in the $CHF_3/H_2/Ar$ plasma system
M_{HF} = mole fraction of HF (%)
M_{SiF_4} = mole fraction of SiF_4 (%)
M_{COF_2} = mole fraction of COF_2 (%)
$M_{CH_2F_2}$ = mole fraction of CH_2F_2 (%)
M_{CH_3F} = mole fraction of CH_3F (%)
M_{CF_4} = mole fraction of CF_4 (%)

Literature Cited

(1) Noto, T.; Babushok, V.; Burgess, D. R., Jr.; Iiamins, A.; Tsang, W.; Miziolek, A. Effect of Halogenated Flame Inhibitors on C_1-C_2 Organic Flames, In *International Twenty-Sixth Symposium on Combustion*; The Combustion Institute, 1996; p 1377.

(2) Linteris, G. T.; Truett, L. Inhibition of Premixed Methane-Air Flames by Fluoromethanes. *Combust. Flame* **1996**, *105*, 15.

(3) Babushok, V.; Noto, T.; Burgess, D. R., Jr.; Iiamins, A.; Tsang, W. Influence of CF_3I, CF_3Br and CF_3H on the High-Temperature Combustion of Methane. *Combust. Flame* **1996**, *107*, 351.

(4) Hayman,G. D.; Derwent, R. G. Atmospheric Chemical Reactivity and Ozone-Forming Potentials of Potential CFC Replacements. *Environ. Sci. Technol.* **1997**, *31*, 327.

(5) Holmes, K. J.; Ellis, J. H. Potential Environmental Impacts of Future Halocarbon Emissions. *Environ. Sci. Technol.* **1996**, *30*, 348A.

(6) Smith, B. K.; Sniegowski, J. J.; Lavigne, G.; Brown, C. Thin Teflon-Like Films for Eliminating Adhesion in Released Polysilicon Microstructure. *Sensor Actuat. A* **1998**, *70*, 159.

(7) Schmidt, I.; Benndorf, C. Mechanisms of Low-Temperature Growth of Diamond Using Halogenated Precursor-Gases. *Diam. Relat. Mater.* **1998**, *7*, 266.

(8) Leech, P. W. Reactive Ion Etching of Piezoelectric Materials in CF_4/CHF_3 Plasma. *J. Vac. Sci. Technol. A* **1998**, *16*, 2037.

(9) Basak, D.; Verdu, M.; Montojo, M. T.; Sanchezgarcia, M. A.; Sanchez, F. J.; Munoz, E.; Calleja, E. Reactive Ion Etching of GaN Layers Using SF_6. *Semicond. Sci. Technol.* **1997**, *12*, 1654.

(10) Hartz, C. L.; Bevan, J. W.; Jackson, M. W.; Wofford, B. A. Innovative Surface Wave Plasma Reactor Technique for PFC Abatement. *Environ. Sci. Technol.* **1998**, *32*, 682.

(11) Mocella, M. T. Environmental Issues in Plasma Processing: A Review of Technologies for PFC Emission Control. *SEMICON Europa* **1997**.

(12) Mocella, M. T. PFC Recovery: Issues, Technologies, and Considerations for Post- Recovery Processing. Presented at the Global Semiconductor Industry Conference on PFC Emission Control, Monterey, CA, April, 1998.

(13) Eliasson, B.; Kogelschatz, U. Nonequilibrium Volume Plasma Chemical Processing. *IEEE Trans. Plasma Sci.* **1991**, *19*, 1063.

(14) Hsieh, L. T.; Lee, W. J.; Li C. T.; Chen, C. Y.; Wang, Y. F.; Chang, M. B. *J. Chem. Technol. Biotechnol.* **1998**, *73*, 432−442.

(15) Lee, W. J.; Chen, C. Y.; Lin, W. C.; Wang, Y. T.; Chin, C. J. Phosgene Formation from the Decomposition of 1,1-$C_2H_2Cl_2$ Contained Gas in an RF Plasma Reactor. *J. Hazard Mater.* **1996**, *48*, 51.

(16) *PFC Emissions Reduction from Semiconductor Processing Tools: Sixth Status Report on Technology and Industry Activities*; Du-Pont, Technical Information: Jan: 1998.

(17) Howard, A. L.; Yoo, W. J.; Taylor, L. T.; Schweighardt, F. K.; Emery, A. P.; Chesler, S. N.; MacCrehan, W. A. Supercritical Fluid Extraction of Environmental Analytes Using Trifluoromethane. *J. Chromatogr. Sci.* **1993**, *31*, 401.

(18) Hsieh, L. T.; Lee, W. J.; Chen, C. Y.; Chang, M. B.; Chang, H. C. Converting Methane by Using an RF Plasma Reactor. *Plasma Chem. Plasma Process.* **1998**, *18*, 215.

(19) Biederman, H.; Osada, Y. *Plasma Polymerization Processes*, Elsevier Science Publishers: New York, 1992.

(20) Breitbarth, F. W.; Berg, D.; Dumke, K.; Tiller, H.-J. Investigation of the Low-Pressure Plasma-Chemical Conversion of Fluorocarbon Waste Gases. *Plasma Chem. Plasma Process.* **1997**, *17*, 39.

(21) Box, G. E. P.; Hunter, W. G.; Hunter, J. S. *Statistics for Experiments*; John Wiley & Sons: New York, 1978.

(22) Manos, D. M.; Flamm, D. L. *Plasma Etching: An Introduction*; Academic Press: New York, 1989.

(23) Boenig, H. *Fundamentals of Plasma Chemistry and Technology*; Technomic Publishing Co., Inc.: Basel, Switzerland, 1988.

(24) Yamamoto, T.; Jiang, B. J.-L. *IAS '96: Conference Record of the 1996 IEEE. Industry Application. Conference: 31st IAS Annual Meeting*, San Diego, CA, Oct. 6−10, 1996; IEEE: Piskataway, NJ, 1996; p 1830.

(25) Chapman, B. *Glow Discharge Processes*; John Wiley & Sons: New York, 1980.

(26) Sekiguchi, H.; Honda, T.; Kanzawa, A. Thermal Plasma Decomposition of Chlorofluorocarbons. *Plasma Chem. Plasma Process.* **1993**, *13*, 463.

(27) Lide, D. R. *CRC Handbook of Chemistry and Physics*; CRC Press, Inc.: Boca Raton, FL, 1994.

(28) Burgess, D. R., Jr.; Zachariah, M. R.; Tsang, W.; Westmoreland, P. R. *Thermochemical and Chemical Kinetic Data for Fluorinated Hydrocarbons*; NIST Technical Note 1412; NIST: Washington, DC, 1995, 1.

(29) Saso, Y.; Zhu, D. L.; Wang, H.; Law, C. K.; Saito, N. Laminar Burning Velocities of Trifluoromethane-Methane Mixtures: Experiment and Numerical Simulation. *Combust. Flame* **1998**, *114*, 457.

(30) Rossnagel, S. M.; Cuomo, J. J.; Westwood, W. D. *Handbook of Plasma Processing Technology*; Noyes Publications: Park Ridge, NJ, 1990.

(31) Roth, J. R. *Industrial Plasma Engineering, Volume 1: Principles*; Institute of Physics Publishing: Bristol, Philadelphia, 1995.

(32) Hsieh, L. T.; Lee, W. J.; Chen, C. Y.; Wu, Y. P. G.; Chen, S. J.; Wang, Y. F. Decomposition of Methyl Chloride by Using an RF Plasma Reactor. *J. Hazard Mater.* **1998**, *B63*, 69.

Received for review January 19, 1999
Revised manuscript received April 26, 1999
Accepted July 17, 1999

IE9900519